Available online at www.sciencedirect.com
ScienceDirect
Trans. Nonferrous Met. Soc. China 24(2014) 360−367
Transactions of Nonferrous Metals Society of China
www.tnmsc.cn

Fretting wear behavior of Inconel 690 in hydrazine environments

Xiao-yu ZHANG, Ping-di REN, Jin-fang PENG, Min-hao ZHU

National Key Laboratory of Traction Power, Southwest Jiaotong University, Chengdu 610031, China

Received 14 January 2013; accepted 26 May 2013

Abstract: The friction and wear behaviors of Inconel 690 flat against Si_3Ni_4 ball were investigated using a hydraulic fretting test rig equipped with a liquid container device. The loads of 20−80 N, reciprocating amplitudes of 80−200 μm and two different environments (distilled water and hydrazine solution at temperatures from 25 to 90 °C) were selected. The results show that the ratio of F_t/F_n is lower in distilled water than that in hydrazine solution at the same temperature in the slip regime. Both the ratio of F_t/F_n and wear volume gradually increase with increasing medium temperature under the given normal load and displacement amplitude. Besides the displacement amplitude and load, temperature also plays an important role for wear behavior of Inconel 690 material. The increase of temperature could reduce the concentration of dissolved oxygen, and promote the absorption reaction of hydrazine and dissolved oxygen. As a result, the oxidative corrosion rate is obviously lowered. Abrasive wear and delamination wear are the main mechanisms of Inconel 690 in distilled water. However, in hydrazine solution the cracks accompanied by abrasive wear and delamination wear are the main mechanisms.

Key words: fretting wear; steam generator; Inconel 690; delamination wear

1 Introduction

Fretting is a wear phenomenon occurring when two contact surfaces are subjected to a small amplitude oscillatory movement, which can accelerate crack nucleation of working components to lead to premature catastrophic failures [1,2]. Fretting corrosion is a fretting model in the electrolytes and other corrosive media where the combined effects of corrosion and abrasion occur in the complex friction process [3]. Steam generator is the major equipment of nuclear power systems, and heat exchanger tube is a key component of the steam generator. Inside steam generators of nuclear power plants, flow-induced vibrations usually cause a relatively small amplitude oscillatory movement between heat exchanger tubes and supports, where fretting corrosion phenomena might occur due to the combined effects of stress and corrosive media, and these phenomena would lead to a reduction of U-tubes life time [4−6]. The nuclear safety is a matter of concern to the entire world. Fatigue fracture [7], intergranular organization [8], stress corrosion [9], corrosion and protection [10], fretting wear [11−14] and other factors [15−19] for Inconel 690 have been researched using micro-analysis equipment, while relatively less work has been carried out on the fretting corrosion damage and its mechanism.

In this work, the fretting wear and its mechanism of Inconel 690 are studied in distilled water and hydrazine solution environments. The chemical composition is investigated by X-ray photoelectron spectroscopy (XPS) in the debris layer.

2 Experimental

A hydraulic fretting wear test rig was used to test the fretting wear behaviours of Inconel 690 alloy under a contact configuration of ball-on-flat. As shown in Fig. 1, the ball specimen was fixed at the upper holder, and moved with the piston of the hydraulic system. The flat specimen was fixed on the lower holder, which was mounted on the specimen chamber. The friction force was measured by sensor of load cell. Cyclic movement between the contact pairs was measured and controlled by the extensometer and its control circuit. The normal load (F_n) was applied on the clamp of the ball by a weight set through a wire. During the fretting test, the variation of tangential force (F_t) versus displacement (D) as a function of fretting cycles (N) was recorded.

Foundation item: Project (51075342) supported by the National Natural Science Foundation of China
Corresponding author: Ping-di REN; Tel: +86-28-87600226; E-mail: rpd@swjtu.edu.cn
DOI: 10.1016/S1003-6326(14)63069-7

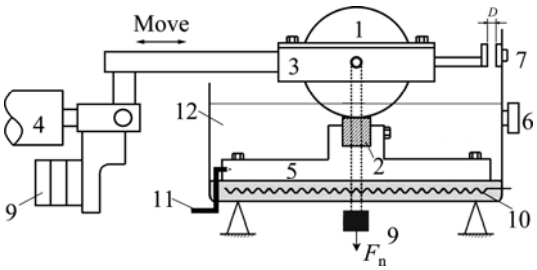

Fig. 1 Fretting wear test rig: 1—Ball specimen; 2—Flat specimen; 3—Upper holder; 4—Piston of hydraulic system; 5—Lower holder; 6—Sensor of load cell; 7—Extensometer; 8—Weight set through a wire; 9—Counterbalance weight; 10—Heater; 11—Thermocouple; 12—Media

The specimens of Inconel 690 alloy were machined to a size of 10 mm×10 mm×20 mm, and the surfaces were carefully polished to a final roughness (R_a) of about 0.02 μm. Si_3N_4 ceramics balls with a diameter of 40 mm and a surface roughness (R_a) of 0.02 μm were used as the counterparts. Prior to the fretting tests, the specimens were ultrasonically cleaned with acetone and thoroughly dried. The chemical composition and mechanical properties of the Inconel 690 alloy and Si_3N_4 ceramics are shown in Tables 1−4. The microstructure of this alloy is completely austenitic, as shown in Fig. 2.

Table 1 Chemical composition of Inconel 690 alloy (mass fraction, %)

Cr	Fe	C	Si	Mn	Ti	P	S	Ni
29	11	0.22	0.28	0.29	0.28	0.006	0.0008	Bal.

Table 2 Main mechanical properties of Inconel 690 alloy

Yield strength /MPa	HRB	Tensile strength/MPa	Modulus of elasticity/GPa
310	85	734	110

Table 3 Chemical composition of Si_3N_4 (mass fraction, %)

Si_3N_4	N	Ca	O	C	Al	Fe	Mn
≥90	≤36	0.25	1.5	0.3	0.25	0.25	0.3

Table 4 Main mechanical properties of Si_3N_4

Compressive strength/MPa	Fracture toughness, K_{IC}/(MPa·m$^{1/2}$)	HRB	Modulus of elasticity/GPa
700	6.7	80	280

The experimental parameters for the fretting wear tests were described as follows: normal load (F_n) of 20, 50 and 80 N, displacement amplitude (D) of 80, 150 and 200 μm at constant frequency of 2 Hz, number of cycles (N) from 1 lasting up to 2×10^4. The fretting wear tests were conducted in distilled water and hydrazine environments, respectively. Three different environments

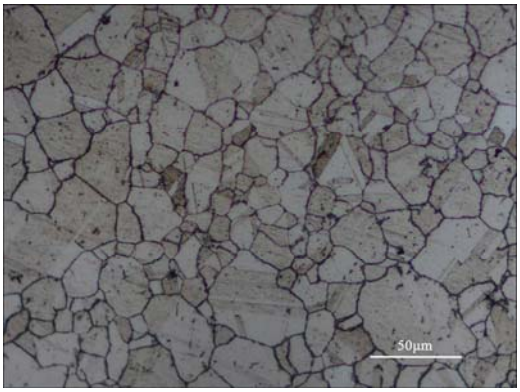

Fig. 2 Microstructure of Inconel 690 alloy

with temperatures of 25, 60 and 90 °C were heated by the lower specimen due to thermal conductivity. In order to maintain the setting temperature, these environments were preheated for 20 min to decrease the differences between the actual and the setting temperature before each test. After the fretting wear tests, pH value of hydrazine solution at 25, 60 and 90 °C were 9.55, 9.03 and 8.443, respectively, according to a pH value detector.

After the fretting wear tests, the morphologies of the worn scars were examined by scanning electron microscopy (SEM, Quanta2000), and chemical compositions were analyzed by X-ray photoelectron spectroscopy (XPS, PHI-5702).

3 Results and discussion

3.1 Friction logs

Friction forces varying with the displacement amplitude (F_t−D curves) are the basic information obtained from the fretting wear tests. According to the variation of F_t−D curves as a function of the number of cycles (F_t−D−N curves, usually named fretting logs), three fretting running regimes [20,21], i.e. partial slip regime (PSR), mixed fretting regime (MFR) and slip regime (SR), are observed. Under a given normal load of 80 N, F_t−D−N curves of Inconel 690 at different displacement amplitudes are shown in Fig. 3. When D=80 and 200 μm (Figs. 3(a) and (b)), all F_t−D curves are open quasi-rectangular, which is the characteristic of slip regime. Relative slip is more obvious under high displacement amplitude.

3.2 F_t/F_n curves

Figure 4 shows the evolution of F_t/F_n (ratio of tangential force to normal force) curves as a function of the number of cycles under different angular displacements. It can be found that the F_t/F_n curves display significantly different evolution in different fretting running regimes. According to the tests, a more

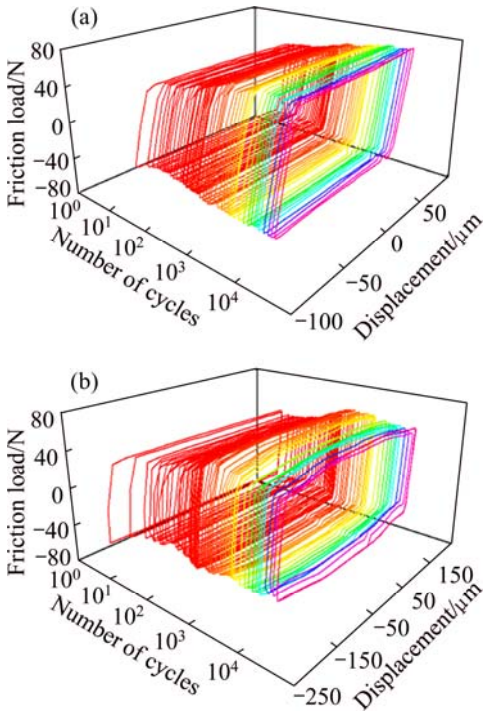

Fig. 3 Fretting logs of Inconel 690 in hydrazine solution of 90 °C under normal load of 80 N: (a) D=80 μm; (b) D=200 μm

complex evolution process of the curve of the ratios of F_t/F_n is presented in the slip regime (D≥80 μm), five stages can be observed, i.e., initial stage, ascending stage, peak-value stage, descending stage and steady stage. The ratio of F_t/F_n is usually low at the early wear stage and then increases rapidly due to the increase of adhesion and abrasion induced by the direct contact between Inconel 690 and Si_3N_4 ceramics. After a lesser number of cycles, the ratio of F_t/F_n quickly increases to a peak value. During the ascent of the curve, metallic particles are detached and ground to form the oxidative third-bodies. After the peak value, the ratio of F_t/F_n slowly decreases owing to load-carrying by the third-bodies taken part in. At the last stage, a balance between continuous formation and overflow of debris is obtained, the ratio of F_t/F_n gradually maintains a steady state, and fretting enters a stable period. The ratio of F_t/F_n is higher in hydrazine solution than that in distilled water under the same conditions (Fig. 4). Under the same displacement amplitude condition, the steady ratio of F_t/F_n decreases with the increase of the normal load and gradually becomes stable. The steady value of F_t/F_n ratio decreases with the increasing of displacement amplitude under a given normal load; while it increases with the increasing of medium temperature under the given displacement amplitude and normal load (Fig. 5).

3.3 Morphologies of wear scars

The fretting track morphologies, as revealed by SEM images, are shown in Figs. 6 and 7 for the tests

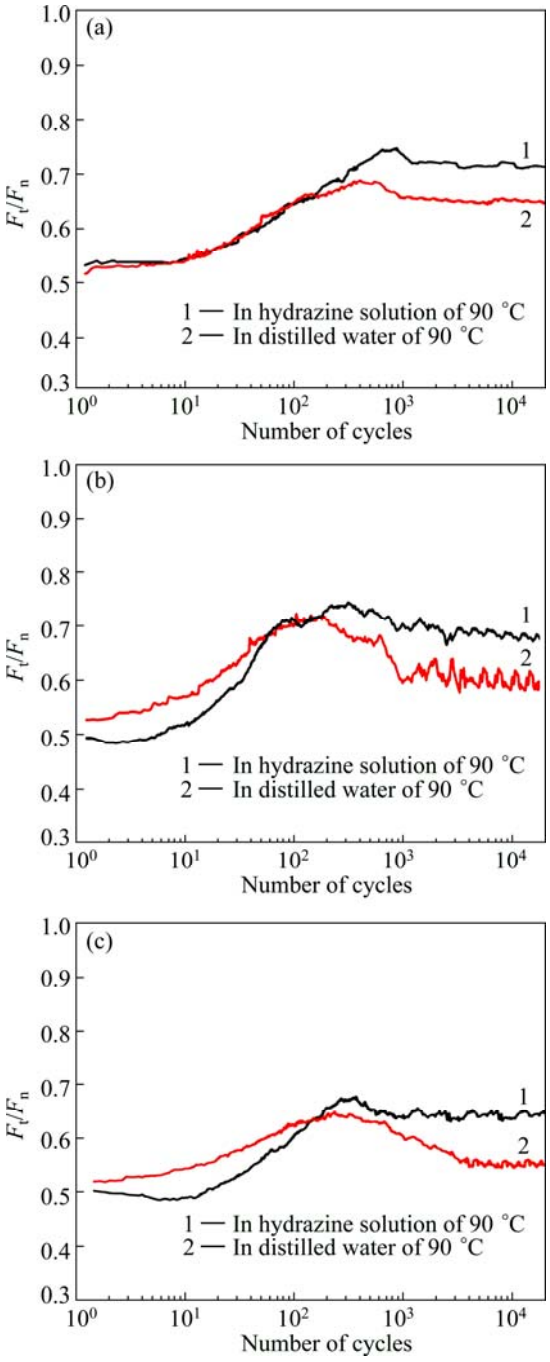

Fig. 4 Ratio of F_t/F_n of Inconel 690 as function of number of cycles at 80 N: (a) D=80 μm; (b) D=150 μm; (c) D=200 μm

performed in distilled water and hydrazine solution, respectively. Abrasion grooves are observed in distilled water and hydrazine solution tracks of the Inconel 690, indicating excessive plastic deformation of Inconel 690. The distilled water track on Inconel 690 (Fig. 6) is covered by a compacted debris layer that seems to protect the surface of the material from further wear. There are areas observed in the track that are not influenced by the fretting test. Wear rate is accelerated with the increase of medium temperature. The debris

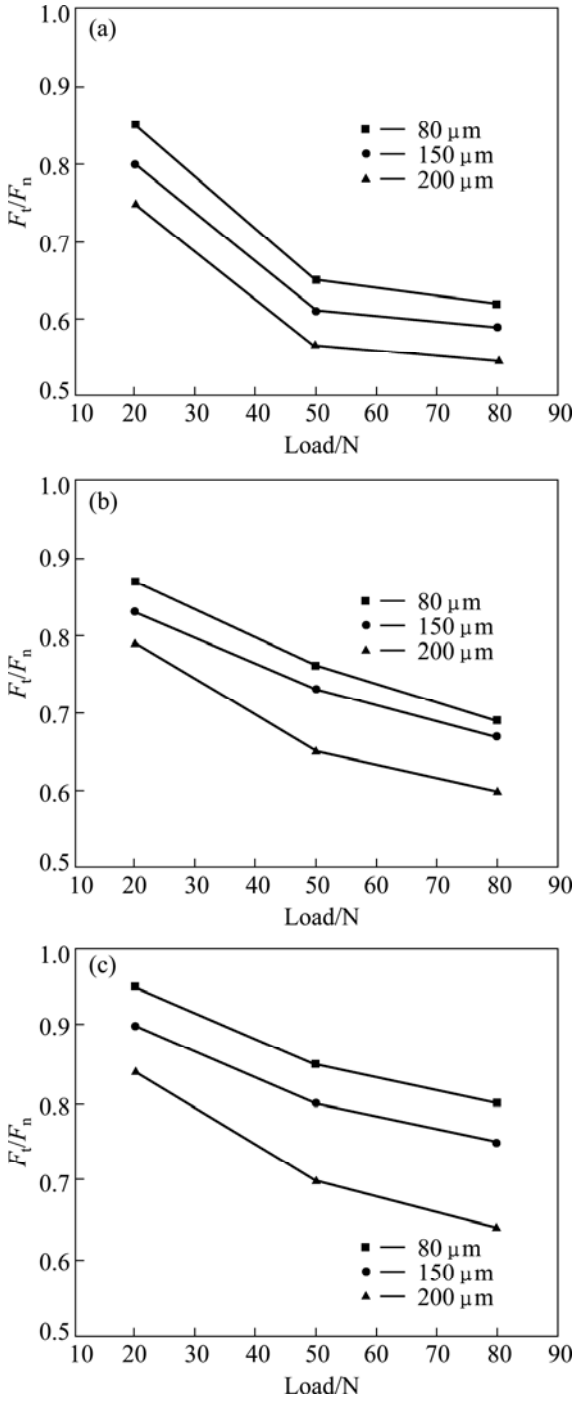

Fig. 5 Ratio of F_t/F_n versus normal load under different amplitudes in distilled water: (a) 25 °C; (b) 60 °C; (c) 90 °C

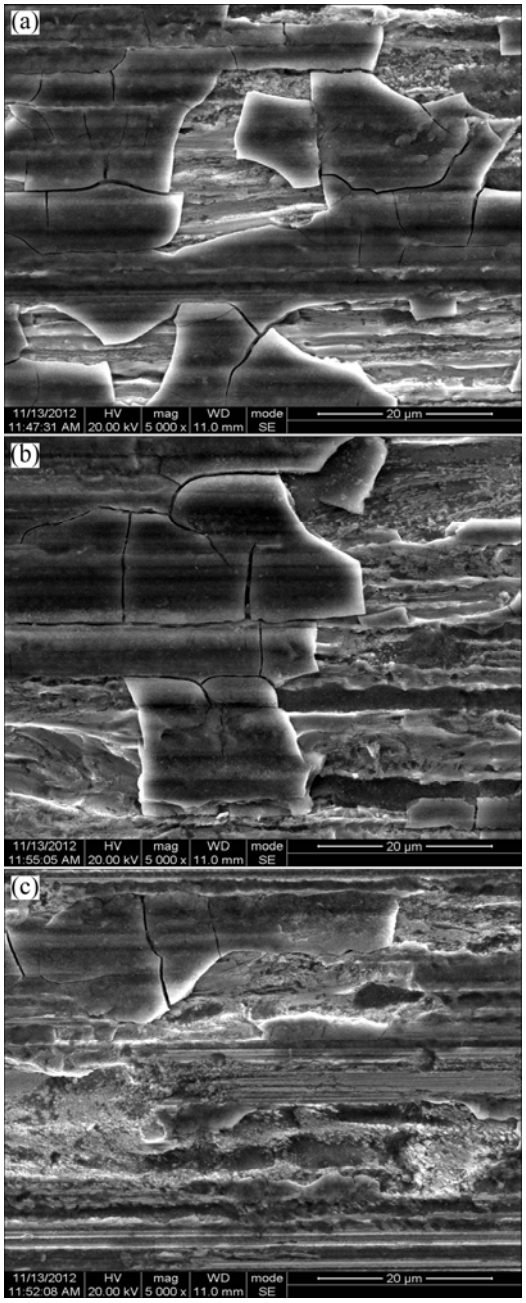

Fig. 6 SEM images of central zone of wear scars in distilled water when F_n=80 N, D=200 μm at different temperatures: (a) 25 °C; (b) 60 °C; (c) 90 °C

particles adhere at the contact area of the distilled water track. A deformed and abraded debris layer is observed on the worn surface (Figs. 6(a) and (b)). Abrasion is promoted by debris particles detached from Inconel 690, as shown in Fig. 6. The debris material is concentrated at the contact zone of the track. A large amount of debris is transformed into a flow layer. The influence of the cracks on the generation of wear debris is shown in Fig. 7(a). The significant abrasion grooves, plastic deformation, and cracks (Figs. 7(b) and (c)) due to the combined effect of wear rate, stress, and chemistry are observed on the worn surface in hydrazine solution. Therefore, the abrasive wear and delamination wear are the main mechanisms of Inconel 690 in distilled water. However, in hydrazine solution, the cracks accompanied by abrasive wear and delamination wear are the main mechanisms.

The depth of wear trace could be calculated according to the width of wear trace obtained from the optical morphologies. According to Fig. 8(a), the depths

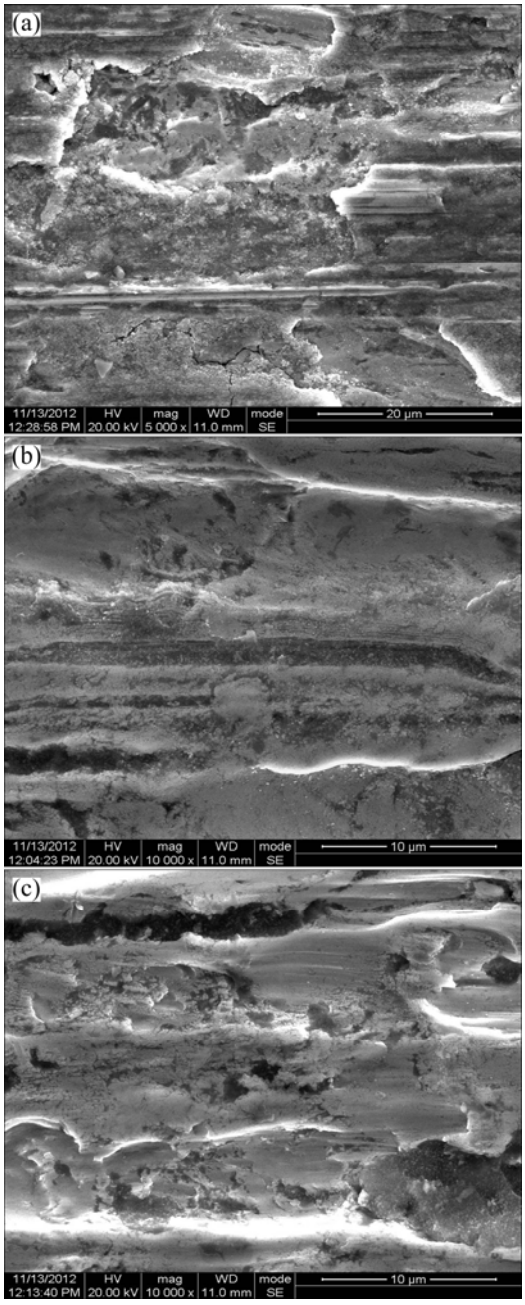

Fig. 7 SEM images of typical wear scars in hydrazine solution when F_n=80 N, D=200 μm at different temperatures: (a) 25 °C; (b) 60 °C; (c) 90 °C

of wear traces in the SR increase with the increase of displacement amplitudes under a given normal load. Wear depth increases due to the increase of the normal load under a given displacement amplitude in distilled water of 90 °C. The depth of wear scars also increases with the solution temperature increasing under a given displacement amplitude. As the solution temperature increases, the area and depth of the wear scars increase with the same normal load in hydrazine solution, as shown in Fig. 8(b). The results reveal that temperature, besides the displacement amplitude and normal load, is

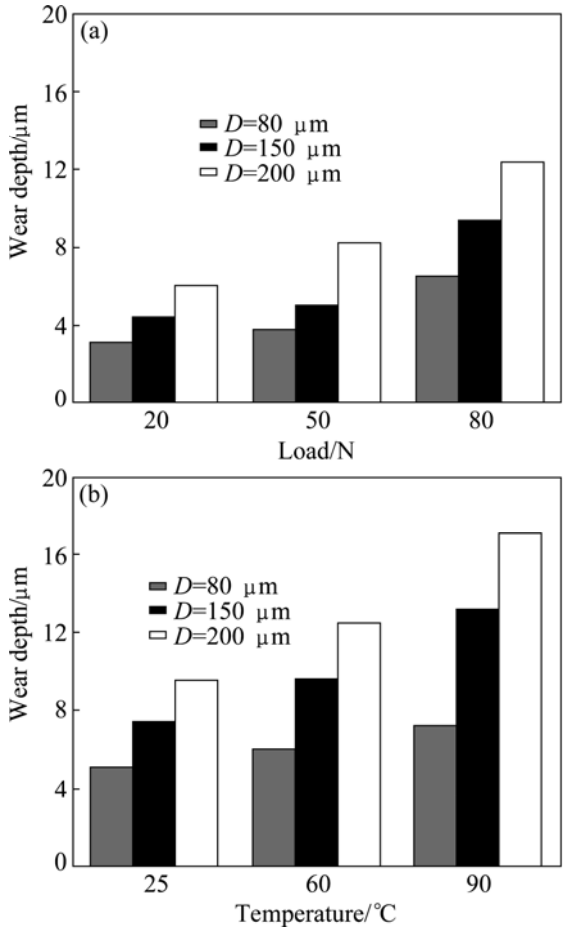

Fig. 8 Depth of wear traces versus normal loads and temperatures in two different environments: (a) In distilled water of 90 °C; (b) In hydrazine solution, F_n=80 N

the major factor affecting fretting wear (Fig. 8(b)). Increasing medium temperature, the dissolved oxygen concentration is reduced in distilled water. On the one hand, increasing temperature promotes the absorption reaction of hydrazine and dissolved oxygen, and the oxidative corrosion rate is lower obviously. On the other hand, the compactness and stability of the oxide films in hydrazine solution are weakened simultaneously. Hence fretting wear becomes more serious.

3.4 Composition of wear debris

Figure 9 shows the composition profiles of the main elements of Inconel 690 at the worn zone in different environments. For fretting tests in distilled water, the oxygen content in the debris layer decreases slowly with the increase of sputtering depth and gradually becomes stable. The nickel content first increases and then decreases with the increase of sputtering depth and tends to be stable. Iron and chrome contents increase slowly with increasing the sputter depth and becomes stable (Fig. 9(a)). For fretting tests in hydrazine solution, the oxygen content decreases with the increase of sputtering

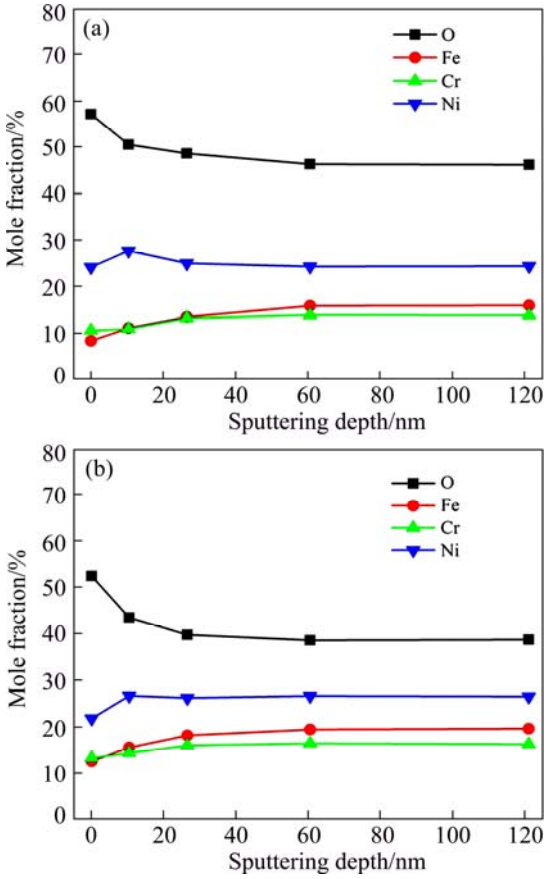

Fig. 9 Composition depth profiles obtained from XPS analysis for wear scar zone on Inconel 690 after fretting at a passive potential of 0.5 V when F_n=80 N, D=200 μm: (a) In distilled water of 60 °C ; (b) In hydrazine solution of 60 °C

depth and gradually becomes stable, while iron, nickel and chrome contents increase slightly with the increase of sputtering depth (Fig. 9(b)).

The oxygen content in Fig. 9(b) is lower than that in Fig. 9(a). The reason is that the combined effect of hydrazine and temperature promotes the absorption reaction of hydrazine and dissolved oxygen and reduces the concentration of dissolved oxygen. Therefore, the oxidative corrosion rate is lowered obviously. The probable reaction is as follows

$$N_2H_4+O_2\rightarrow N_2+2H_2O \quad (1)$$

The XPS spectra of Cr 2p on the worn surfaces are shown in Fig. 10. For peak fitting analysis of Cr 2p spectra, the Cr 2p spectra at peak binding energy of 577± 0.3 eV and 574±0.3 eV correspond to the formation of Cr and Cr_2O_3, respectively [22].

The XPS spectra of Ni 2p on the worn surfaces are shown in Fig. 11. The Ni 2p spectrum is decomposed according to the procedure described in Ref. [23]. On the worn surfaces of Inconel 690, nickel is presented in the form of Ni^{3+}, Ni^{2+} and Ni^0 (E_b=856.5±0.3 eV, 854.2±0.3 eV and 852.5±0.3 eV, respectively) as in the composition of Ni_2O_3, NiO, and Ni (Fig. 11(a)), two other components (and the associated satellites) are defined: a signal from metallic Ni in the alloy at binding energy of 852.5± 0.3 eV (satellite at 858.6±0.4 eV with respect to the main signal) and another Ni oxide (NiO) at binding energy of 854.2±0.3 eV (Figs. 11(b) and (c)).

The XPS spectra of Fe 2p on the worn surfaces are shown in Fig. 12. The shape of the band and the binding energies of Fe 2p electrons suggest that iron presents in the form of Fe^{3+}, Fe^{2+} and Fe^0 (E_b=716.4±0.3 eV, 712.4± 0.3 eV and 707±0.3 eV, respectively). It forms Fe_2O_3, Fe_3O_4 and Fe [24].

As mentioned above, composition and structure are important factors affecting the fretting occurrence, development and control in the friction process [25]. The oxides and elementary substances of the three main alloying elements (Ni, Cr and Fe) are formed in the debris layer. Also, the oxide content which decreases with the increase of temperature is lower in hydrazine solution than that in distilled water. So, temperature plays an important role in the fretting wear. Increasing temperature could reduce the concentration of dissolved

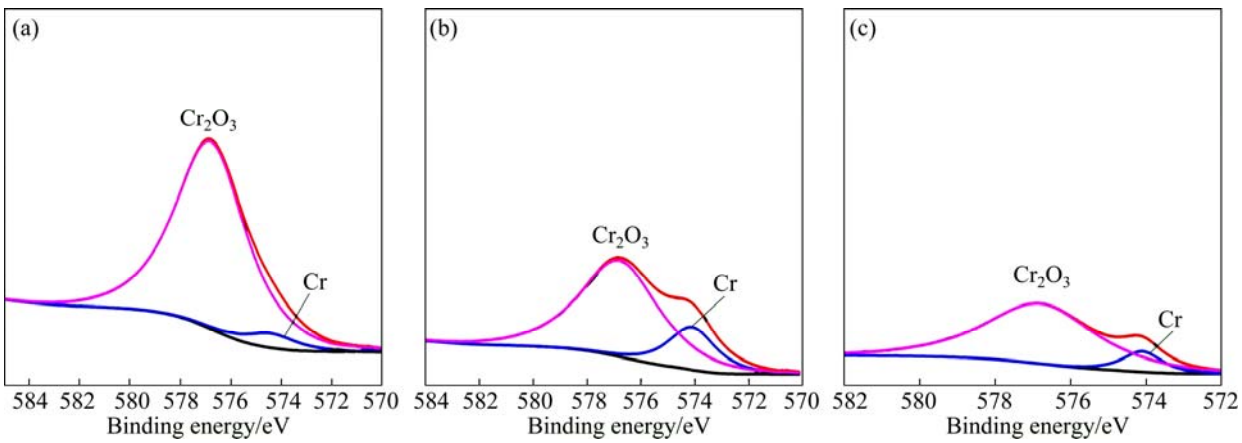

Fig. 10 XPS spectra of Cr $2p_{3/2}$ for wear scar zone on Inconel 690 for sputtering depth of 121.26 nm when F_n=80 N, D=200 μm: (a) In distilled water of 60 °C; (b) In hydrazine solution of 60 °C; (c) In hydrazine solution of 90 °C

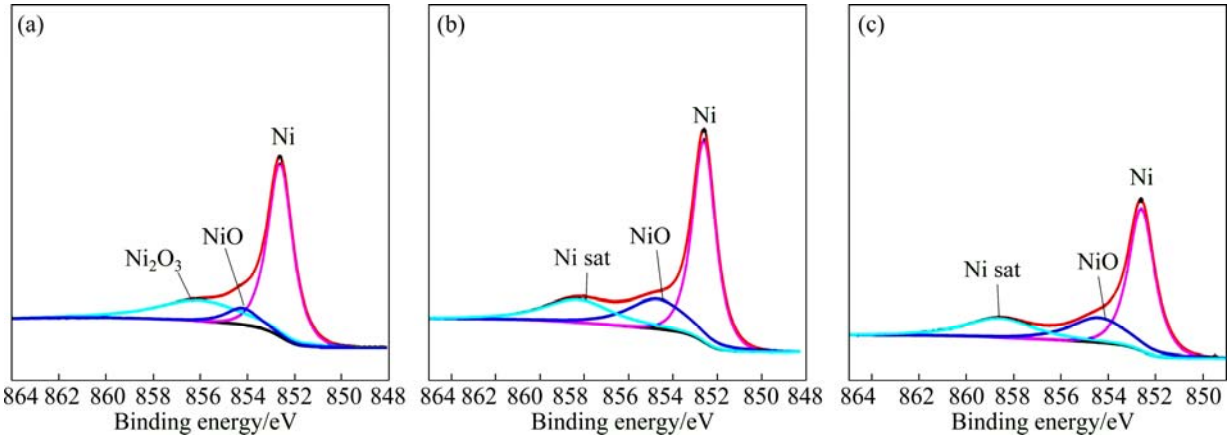

Fig. 11 XPS spectra of Ni $2p_{3/2}$ for wear scar zone on Inconel 690 for sputtering depth of 121.26 nm when F_n=80 N, D=200 μm: (a) In distilled water of 60 °C; (b) In hydrazine solution of 60 °C; (c) In hydrazine solution of 90 °C

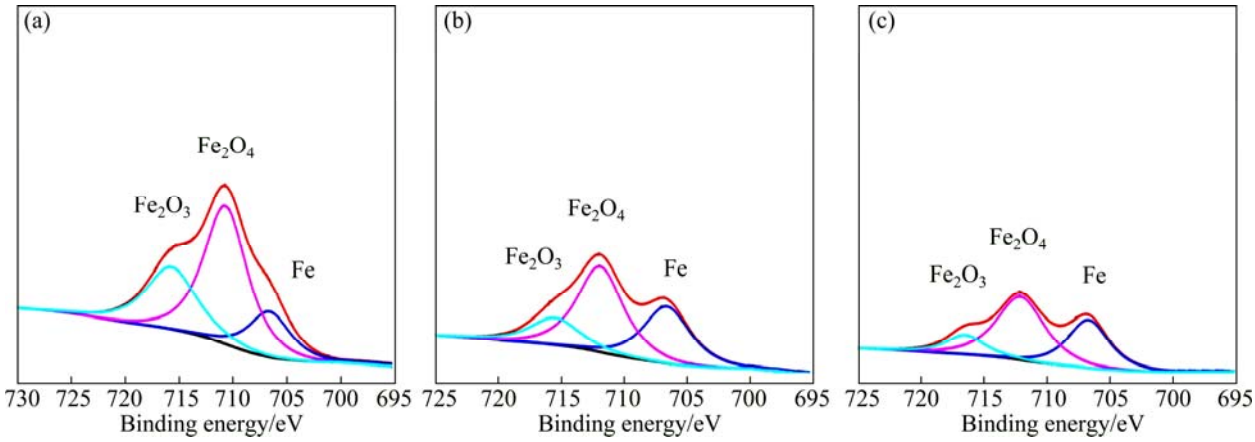

Fig. 12 XPS spectra of Fe $2p_{3/2}$ for wear scar zone on Inconel 690 for sputtering depth of 121.26 nm when F_n=80 N, D=200 μm: (a) In distilled water of 60 °C; (b) In hydrazine solution of 60 °C; (c) In hydrazine solution of 90 °C

oxygen in distilled water, promote the absorption reaction of hydrazine and dissolved oxygen, and the oxidative corrosion rate is obviously lowered. In fact, a large number of metal oxide films with good compactness and stability are produced on the worn surface in distilled water. The wear of materials is alleviated due to avoiding the direct contact between materials and media, so that the materials are protected from serious wear. It indicates that the oxide film formation and the compactness and stability of the films depend on temperature and media. With the increasing solution temperature, the absorption reaction of hydrazine and dissolved oxygen is promoted, oxidative corrosion rate is decreased, but the compactness and stability of the oxide films are significantly lower [26]. Therefore, wear becomes more serious.

4 Conclusions

1) The ratio of F_t/F_n is lower in distilled water than that in hydrazine solution at the same temperature, and the wear volume and the ratio of F_t/F_n increase with the increase of solution temperature under a given normal load and displacement amplitude in the slip regime.

2) Besides the displacement amplitude and normal load, temperature also plays an important role in the fretting wear. Increasing temperature promotes the absorption reaction of hydrazine and dissolved oxygen, and obviously reduces oxidative corrosion rate, but the compactness and stability of the oxide films are weakened. So, fretting wear becomes more serious.

3) The abrasive wear and delamination wear are the main mechanisms of Inconel 690 in distilled water. However, in hydrazine solution the cracks accompanied by abrasive wear and delamination wear are the main mechanisms.

References

[1] WATERHOUSE R B. Fretting fatigue [J]. International Materials Reviews. 1992, 37(3): 77−98.

[2] WATERHOUSE R B. Fretting wear [M]//ASM Hand book: Friction,

lubrication and wear technology. Vol. 18. Clevelaud, OH: ASM International, 1992: 233.
[3] WATERHOUSE R B. Fretting corrosion [M]. Oxford: Pergamon Press, 1972.
[4] LOW M B J. Fretting problems and some solutions in power plant machinery [J]. Wear, 1985, 106(1−3): 315−336.
[5] SHERWIN M P, TAYLOR D E, WATERHOUSE R B. An electrochemical investigation of fretting corrosion in stainless steel [J]. Corrosion Science, 1971, 11(6): 419−429.
[6] VIJH A K. Observations on: The fretting corrosion of a number of pure metals in sodium chloride solutions [J]. Corrosion Science, 1974, 14(11): 613−615.
[7] KWONA J D, JEUNGB H K, CHUNGA I S, YOON D H, PARK D K. A study on fretting fatigue characteristics of Inconel 690 at high temperature [J]. Tribology International, 2011, 44(11): 1483−1487.
[8] RODRIGUEZA J G G, CASALESB M, MEDINA M A E, CHAVEZ C A, IZQUIERDO G, GUARDIAN R. Microstructural evolution of alloy 690 during sensitization at 700 °C [J]. Material Characterization, 2003, 51(5): 309−314.
[9] MENG F J, WANG J Q, HAN E H, KE W. The role of TiN inclusions in stress corrosion crack initiation for alloy 690TT in high temperature and high-pressure water [J]. Corrosion Science, 2010, 52(3): 927−932.
[10] BALDRIDGE T, POLING G, FOROOZMEHR E, KOVACEVIC R, METZ T, KADEKAR V, GUPTA M C. Laser cladding of Inconel 690 on Inconel 600 super alloy for corrosion protection in nuclear applications [J]. Optics and Lasers in Engineering, 2013, 51(3): 180−184.
[11] JEONG S H, CHO C W, LEE Y Z. Friction and wear of Inconel 690 for steam generator tube in elevated temperature water under fretting condition [J]. Tribology International, 2005, 38(3): 283−288.
[12] ILSUP C, MYUNGHO L. An experimental study on fretting wear behavior of cross-contacting Inconel 690 tubes [J]. Nuclear Engineering and Design, 2011, 241(10): 4103−4110.
[13] RUBIOLO P R, YOUNG M Y. On the factors affecting the fretting-wear risk of PWR fuel assemblies [J]. Nuclear Engineering and Design, 2009, 239(1): 68−79.
[14] ZHANG Xiao-yu, REN Ping-di, ZHANG Ya-fei, ZHU Min-hao, ZHOU Zhong-rong. Fretting wear behavior of Incoloy800 alloy at high temperature [J]. The Chinese Journal of Nonferrous Metals, 2010, 20(8): 1545−1551. (in Chinese)
[15] YOUNG B A, GAO X S, SRIVATSAN T S, KING P J. There sponse of alloy 690 tubing in a pressurized water reactor environment [J]. Materials and Design, 2007, 28(2): 373−379.
[16] ATTIA M H. Fretting fatigue and wear damage of structural components in nuclear power stations fitness for service and life management perspective [J]. Tribology International, 2006, 39(10): 1294−1304.
[17] FERNG Y M, FAN C N, PEI B S, LI H N. Predicting the accumulated number of plugged tubes in a steam generator using statistical methodologies [J]. Annals of Nuclear Energy, 2008, 35(10): 1912−1918.
[18] REN Ai, LI Cheng-tao, LIU Fei-hua, LI Yan, LI Xiao-gang. Effect of Cl^- on corrosion behavior of alloy 690 in high temperature and high pressure water solution [J]. The Chinese Journal of Nonferrous Metals, 2012, 22(4): 1082−1087. (in Chinese)
[19] BIROL Y. Inconel 617 and Stellite 6 alloys for tooling in thixoforming of steels [J]. Transactions of Nonferrrous Metals society of China, 2010, 20(9): 1656−1662.
[20] ZHOU Z R, VINCENT L. Mixed fretting regime [J]. Wear, 1995, 181−183(11−12): 531−536.
[21] ZHOU Z R, NAKAZAWA K, ZHU M H, MARUYAMA N, KAPSA P, VINCENT L. Progress in fretting maps [J]. Tribology International, 2006, 39(10): 1063−1073.
[22] PAYNE B P, BIESINGER M C, MCINTYER N S. X-ray photoelectron spectroscopy studies of reactions on chromium metal and chromium oxide surfaces [J]. Journal of Electron Spectroscopy and Related Phenomena, 2011, 184(1−2): 29−37.
[23] GROSVERNOR A P, BIESINGER M C, SMART R S C, MCINTYER N S. New interpretations of XPS spectra of nickel metal and oxides [J]. Surface Science, 2006, 600(9): 1771−1779.
[24] TORU Y, PETER H. Analysis of XPS spectra of Fe^{2+} and Fe^{3+} ions in oxide materials [J]. Applied Surface Science, 2008, 254(8): 2441−2449.
[25] ZHANG Xiao-yu, REN Ping-di, ZHONG Fa-chun, ZHU Min-hao, ZHOU Zhong-rong. Fretting wear and friction oxidation behavior of 0Cr20Ni32AlTi alloy at high temperature [J]. Transactions of Nonferrrous Metals society of China, 2012, 22(4): 825−830.
[26] HUANG J B, WU X Q, HAN E H. Electrochemical properties and growth mechanism of passive films on alloy 690 in high-temperature alkaline environments [J]. Corrosion Science, 2010, 52(10): 3444−3452.

Inconel 690 在联氨溶液中的磨损行为

张晓宇，任平弟，彭金方，朱旻昊

西南交通大学 牵引动力国家重点实验室 摩擦学研究所，成都 610031

摘　要：在控制法向载荷分别为 20、50 和 80 N，位移幅值分别为 80、150 和 200 μm 的两种不同环境下，以 Si_3N_4 陶瓷球/Inconel690 平面接触的方式，在 PLINT 高温微动试验机上进行微动腐蚀试验，循环次数为 2×10^4。结果表明：在滑移区，当载荷、位移幅值一定时，相同温度联氨溶液中的稳态摩擦因数比其在蒸馏水中高；稳态摩擦因数随溶液的温度增加而增加；磨损体积随溶液温度增加而增加。Inconel 690 在联氨溶液摩擦过程中，磨损程度除受到位移幅值、荷载影响以外，温度对磨损体积有显著影响。温度的增加即降低溶液的溶解氧又促进联胺与溶解氧的吸收反应，起到降低氧化腐蚀的作用。在蒸馏水中 Inconel 690 合金材料的磨损机制主要为磨粒磨损和剥层，而在联氨溶液中其磨损机制主要为裂纹伴随磨粒磨损和剥层。

关键词：微动磨损；蒸汽发生器；Inconel 690；剥层

(Edited by Chao WANG)